Density Functional Response Calculations of Dispersion Coefficients C_6 and C_9 of Closed- and Open-shell Systems

Laura Abella, Jochen Autschbach*

Department of Chemistry
University at Buffalo
State University of New York
Buffalo, NY 14260-3000, USA
Fax: (+) +01-716-645-6963
email: jochena@buffalo.edu

Abstract: Dipole polarizabilities and C_6 and C_9 dispersion coefficients are computed for closed- and open-shell atoms and molecules, using dynamic (time-dependent) density functional (TD-DFT) linear response theory as implemented in the response module of the NWChem quantum chemistry package. The response module is capable of accurate calculations of these properties, based on spin-restricted and spin-unrestricted formalisms. The calculated static polarizabilities and dispersion coefficients are compared to available experimental and other theoretical data. The behavior of the dynamic polarizability at imaginary frequencies is analyzed for differently sized closed- and open-shell systems. An interpolation method enforcing the monotonic decrease of the polarizability with increasing imaginary frequency is beneficial for the integration used to obtain C_6 and C_9. Scaling of the TD-DFT data by ratios of the static polarizability, which can be calculated with a variety of methods, including highly accurate theories, may be used as a leading-order correction.

1 Introduction

Interactions between atoms or molecules outside of the orbital overlap range are governed by van der Waals (vdW) forces. Typically, one distinguishes long-range electrostatic vs. dispersion interactions, with the latter being caused by the dynamic electron correlation. Dispersion interactions are mediated by instantaneous multipole moments in one subsystem inducing instantaneous multipole moments in another subsystem. These interactions are extremely important in chemical, physical and biological systems. With distance R_{AB} between two species (subsystems), A and B, the asymptotic expansion of the nonrelativistic two-body dispersion interaction is in leading order C_6/R_{AB}^6, with relativistic and higher multipole order corrections involving higher powers of $1/R$. C_6 is the coefficient that quantifies the dipole-dipole interactions. There is a corresponding $C_9/(R_{AB}^3 R_{BC}^3 R_{CA}^3)$ term parametrizing the three-body dipole interactions among subsystems A, B, and C. Many studies of C_6 coefficients have been reported for rare gas atoms, alkali-atoms, alkali-metal clusters, diatomic

molecules, alkanes, polycyclic aromatic hydrocarbons, and fullerenes.[1–19] Nevertheless, an accurate determination of dispersion coefficients such as C_6 and C_9 is not simple in general, and far from routine for open-shell systems.

A variety theoretical approaches, such as density functional theory (DFT),[20,21] linear-response time-dependent DFT (TD-DFT),[1,7,12,14,19,22–24] the DFT-based local response dispersion (LRD) method,[25] time-dependent Hartree-Fock (TDHF),[12,17,26] Møller-Plesset perturbation theory (MPPT),[27–29] perturbation theory,[5,30–33] symmetry-adapted perturbation theory (SAPT),[34–38] other correlated wavefunction approaches[39,40] such as coupled cluster (CC) theory[17,29,41–45] and the algebraic diagrammatic construction (ADC),[17] and semi-empirical approximations,[46–54] have been harnessed to calculate polarizabilities and dispersion coefficients. Static polarizabilities of closed- and selected open-shell atoms and small molecules may be computed accurately by quantum chemical techniques.[19,23,25,55] Treating frequency-dependent response is in principle straightforward, but requires additional method development effort. Molecules that are not small and have unpaired electrons remain a challenge in the treatment of response properties in general, including dispersion interactions. Consequently, few reports of dispersion coefficient calculations of such systems—which may be highly relevant in chemistry and materials science—are yet available.

One of us has previously developed a TDDFT dynamic linear response module in the NWChem program,[56–58] which allows for massively parallelized computations of large systems. The response module is capable of calculating dynamic polarizabilities at complex frequencies, to obtain non-singular response near or at resonances.[59] The module was subsequently extended to accommodate spin-unrestricted calculations,[60] which therefore allows for a uniform treatment of closed- and open-shell systems, thus expanding the application range of TDDFT response methodology to chemical, physical and biological systems without or with unpaired spins. Herein, we report calculations of dipole-polarizabilities at purely imaginary frequencies, to determine dispersion coefficients C_6 and C_9 for open- and closed-shell systems by integration of polarizability products along the imaginary frequency axis (see Section 2). Static polarizability benchmark data are also provided. The integration to obtain C_6 and C_9 coefficients is commonly done on a numerical grid of imaginary frequencies $i\omega$ (with ω being real). The polarizability tends to be rapidly decreasing with increasing $i\omega$, and monotonic. We show that the integration to obtain dispersion coefficients can be facilitated by using a cubic interpolation scheme that enforces the monotonic behavior. In the present study, we first test small open- and closed-shell species, then proceed with calculations for larger molecules. The results are rather satisfactory for all of the different systems that were studied.

2 Theoretical and Computational Details

Let the isotropic dipole polarizability of entity (subsystem) A be denoted by α^A. The isotropic polarizability is the average of the principal components of the rank-2 polarizability tensor. For the present study, the dispersion coefficient C_6(A,B) for the rotationally averaged interaction between entity A and B was calculated via the Casimir-Polder expression, in terms of the dynamic (frequency-dependent) polarizability at imaginary frequencies[61,62] Hartree atomic units (au) are used unless noted otherwise. The C_6 coefficient is given as

$$C_6(\mathrm{A,B}) = \frac{3}{\pi}\int_0^\infty \alpha^A(i\omega)\alpha^B(i\omega)\,d\omega \tag{1}$$

Here, ω is a real circular frequency, assumed to be positive, such that the integration in the previous equation is along the positive imaginary axis. At purely imaginary frequencies, the polarizability is purely real. Similar to C_6, the three-body coefficient C_9(A,B,C), which is useful in the modeling of non-additive effects, can be obtained via

$$C_9(\mathrm{A,B,C}) = \frac{3}{\pi}\int_0^\infty \alpha^A(i\omega)\alpha^B(i\omega)\alpha^C(i\omega)\,d\omega. \tag{2}$$

The isotropic part of the polarizability at $\omega = 0$ and nonzero imaginary frequencies $i\omega$ for all systems was computed by using the Kohn-Sham (KS) density functional theory (DFT) dynamic linear response module of the NWChem package[56–58] as released on GitHub.[63] The code allows for response calculations with complex frequencies, and includes recent minor changes to allow polarizability calculations with frequencies that are purely imaginary. The Coulomb attenuation method with the Becke three parameter Lee-Yang-Parr (CAM-B3LYP)[64] hybrid functional, and the Sadlej polarized valence triple zeta (pVTZ)[65] Gaussian-type orbital (GTO) basis set, were employed for most calculations, except where noted otherwise. This functional and basis combination were previously reported to produce accurate static polarizabilities.[66] Test calculations with several other functionals and basis sets were performed for alkali-metal atoms and selected diatomic molecules. Basis sets were obtained from the basis set exchange.[67,68] A response convergence criterion of 10^{-7} was chosen, with the only exception of C_{60} fullerene where a criterion of 10^{-6} was used because of elevated numerical noise related to near linear dependencies with the used basis set. We note that the calculations for the alkali-metal atoms and small molecules required only very modest computational resources. The computational cost of course increases with the size of the system, with the same overall scaling in the code as the utilized (hybrid) Kohn-Sham DFT

approximations, with the C_{60} fullerene being the most demanding system in this study. In part thanks to the favorable scaling on NWChem on parralel architectures, the calculations on the larger systems remain accessible on a modern multi-core processor system.

There are different keywords to specify the perturbation in the input for the NWChem response module. One input value is for the real frequency of the perturbing field. The other input parameter is for a 'damping' or de-phasing constant that broadens the excited states in the response calculations and plays an analogous role to the friction damping of a classical oscillator. When both a frequency and de-phasing constant are provided, the response calculation effectively runs with a complex perturbing frequency, with the imaginary part of the frequency being equal to the de-phasing constant. Thus, electric-field perturbation calculations with purely imaginary frequencies were achieved by setting the real frequency to zero and selecting nonzero damping values ω representing $i\omega$ in the previous equations. The electric dipole moment response then gave $\alpha(i\omega)$.

For most calculations, ω ranged from 0 to 81.92 au on a 15-point frequency grid, with the nonzero frequencies corresponding to a logarithmic grid of 0.01 au times 2^n with $n =$ 0 to 13. Test calculations for the K atom also used a larger logarithmic grid of 0.00001 au times 1.2^n with $n = 0$ to 101, to test grid cut-off errors and different interpolations (vide infra). The monotonic cubic splines Steffen interpolation[69] was used as implemented in the `CubicMonotonicInterpolation` function available in *Mathematica*[70] v. 13 via the Wolfram Function Repository. We additionally verified that this function produces the same results as a *Mathematica* code for the Steffen interpolation that can be found on the StackExchange web site.[71] For comparison, a 12-point Gauss-Legendre quadrature, as applied in several of the works referenced herein,[12,17,43] was also used in the integration tests. Accordingly, the polarizability was calculated for frequencies $i\omega = i\omega_0(1-t)/(1+t)$, with $\omega_0 = 0.3$ au and discrete values of $t \in [-1, 1]$ and associated weights generated for the requested number (12) of Gauss-Legendre quadrature points. This integration was deemed to be reliable in the cited references, 'well beyond [...] three-digit accuracy'.[17]

For small molecules, we used the same experimental ground state structural data as Reference 28. In particular, the bonds lengths for diatomic molecules[72] were as follows (in Å): H_2: 0.741 Å. N_2: 1.098. CN: 1.172. CO: 1.128. NO: 1.151. O_2: 1.208. BeH: 1.343. CaH: 2.002. MgH: 1.731. Li_2: 2.673. Na_2: 3.079. K_2: 3.905 Å. An experimental X-ray diffraction structure was used for the radical cation bicarbazole (BCz)[73] derivative. Structures for other systems were optimized with the PBE0[74] hybrid functional and the def2-SV(P) basis[75,76] using Gaussian (G16).[77]

3 Results and Discussion

3.1 Polarizabilities for alkali-metal atoms and some diatomic molecules

We first examine the static polarizabilities of the alkali-metal atoms Li, Na and K, as well as the diatomic molecules H_2, N_2 and CO, prior to proceeding with calculations for larger systems. We reiterate that the module for linear response theory calculations in NWChem can be employed in spin-restricted as well as in spin-unrestricted fashion. Therefore, the alkali-metal atoms Li, Na and K are good examples for testing this functionality.

For accurate calculations of polarizabilities, especially for small systems, large basis sets with polarization and diffuse functions are necessary. The exchange-correlation (XC) functional and the associated response kernel also play an important role, in property calculations in general and for polarizabilities in particular. Thus, in order to determine the most accurate method to calculate the static polarizabilities, an extensive test of different functionals and basis sets was performed. The results are collected in Table S1 in the Supporting Information (SI). These calculations identified CAM-B3LYP/Sadlej-pVTZ as a suitable choice. As far as functionals with range-separated exchange and a full long-range correction (LC) are concerned, some of the results obtained with LC functionals also agree well with experiments. For example, LC-PBE and LC-PBE0 results agree reasonably well with the experimental polarizability of the Li atom (calc. ∼153-160 atomic units (au) vs. expt. 164 $\pm$ 3.0 au[78]). Results from the similar LC-ωPBE and LC-ωPBE0 functionals also produce results close to the experimental polarizability (Li: 160-165 au for LC-ωPBE and 156-160 au for LC-ωPBE0). The range-separation parameter for the LC functionals was also non-empirically tuned for Li, as described in Reference[79] and works cited therein; however, no dramatic impact on the resulting polarizability was found. We note that for Li the Sadlej basis is the one that works best in conjunction with the LC functionals. For Na, the LC functionals also provide results within the experimental range (for example, 161-165 au from LC-PBE vs. an expt. value of 159.2 $\pm$ 3.4).[78] However, the calculated static polarizabilities for K are somewhat overestimated with the LC functionals. We therefore decided to proceed with the CAM-B3LYP functional, also because of its expected better performance for larger systems.

Table 1 collects the calculated static polarizabilities from the CAM-B3LYP/Sadlej-pVTZ calculations for the alkali-metal atoms Li, Na and K, and the diatomic molecules H_2, N_2 and CO. Available experimental data,[78,80,81] and results from other other theoretical works[1,3–5,7,28] are also provided. In general, the CAM-B3LYP functional with the Sadlej family of basis sets is found to produce accurate results when they are compared with experiments, both here and in the literature.[66] Comparisons with other theoretical data reported in the literature[1,7,28]

shows that our calculated static polarizabilities for K, H_2, N_2 and CO agree as well or better with experiments. Our calculated polarizabilities for the alkali-metal atoms Li and Na are below the experimental references. Some of the functional and basis set combinations that give closer results to the experiment for Li and Na (Table S1) strongly overestimate the polarizability of K, which highlights the challenge of calculating response properties with TDDFT across a variety of systems. The calculation results are overall reasonable, especially when taking into account the good performance of the CAM-B3LYP/Sadlej-pVTZ calculations for K and the diatomic molecules.

3.2 Polarizability integration along the imaginary frequency axis

Calculations for the K atom were used to test the requirements for obtaining accurate dispersion coefficients from numerical integration of $\alpha(i\omega)$. Plots of the polarizability along the imaginary frequency axis are shown in Figure 1. A large, finely spaced logarithmic grid (see Section 2 for details) was compared to the 15-point grid with ca. 80 au cutoff used for most of the calculations (hereafter referred to as the 'standard' grid). The data are representative of $\alpha(i\omega)$ for all systems in our study: From its static limit, $\alpha(i\omega)$ drops initially somewhat Gaussian-like, then goes through an inflection point and drops more slowly for larger fre-

Table 1: Experimental and computational static polarizabilities (in atomic units) of some alkali-metal atoms and diatomic molecules, as well as a comparison with other studies is represented.

Source	Li	Na	K	H_2	N_2	CO
Expt.	164 ± 3.0[a]	159.2 ± 3.4[a]	292.8 ± 6.1[a]	5.4[b]	11.7[b]	13.1[c]
This work[d]	148.8	146.6	290.3	5.4	11.8	13.1
Ref. [4][e]	162.97	157.65	276.89			
Ref. [28][f]	165	166.9	285.2			
Ref. [5][g]	163.7	162.2	286.1	6.7		
Ref. [3][h]	163.7	162.4	287.1			
Ref. [54][i]	164.3	162.8	290.0			
Ref. [1][j]				6.1	12.3	13.7
Ref. [7][k]				5.7	11.9	13.1

[a]Reference 78. [b]Reference 80. [c]Reference 81. [d]CAM-B3LYP/Sadlej-pVTZ. [e] TDDFT-based complete sum-over-states with Slater-type orbital (STO) basis. [f] Møller-Plesset perturbation theory (MPPT) based on the quasi-energy derivative (QED) method using Gaussian-type orbital (GTO) basis. [g] Perturbational approach, configuration interaction (CI) calculation using GTO basis. [h] Configuration interaction (CI) + core polarization potential method with GTO basis. [i] Semi-empirical method using oscillator strength distributions. Numerical simulations. [j] TDDFT with adiabatic local density approximation (ALDA) and STO basis. [k] TDDFT with STO basis.

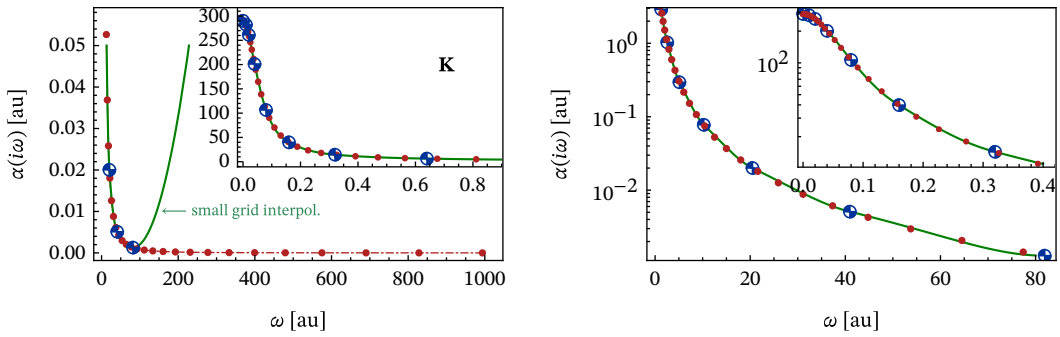

Figure 1: Potassium atom. Left: Isotropic polarizability for imaginary frequencies. Standard grid (large markers) vs. extended fine grid (small markers with dashed-dotted interpolation line) vs. Steffen interpolation (straight line) from the standard grid data. Right: Standard and fine grid data compared to the standard-grid Steffen interpolation, using a logarithmic scale for the vertical axis in the plot.

quencies.

Given the general behavior of $\alpha(i\omega)$, one may take advantage of interpolation methods that use advance knowledge of the monotonic decrease with increasing $i\omega$. We used in this work the monotonic cubic splines interpolation of Steffen.[69] As can be seen from the inset in the left panel of Figure 1, the Steffen interpolation works extremely well. The interpolation function generated from the standard grid of frequency points essentially goes right through the data points from the fine grid. The log-plot of $\alpha(i\omega)$ in the right panel of Figure 1 indicates only minor interpolation errors between the standard grid points. This means that the standard grid with Steffen interpolation will produce reliable integrations for obtaining C_6 and C_9 coefficients.

Integration of $\alpha(i\omega)$ itself between 0 and 81.92 au, as a measure of the accuracy of the grid and the interpolation, gives 35.93 for the Steffen interpolation using the *fine* grid, compared to 36.14 with linear interpolation between the data points from the same grid. The two values are 35.95 and 38.86, respectively, when using the coarser standard grid. The error from using linear as compared to Steffen interpolation is 7.5% for the coarse grid and drops to less than 1% for the fine grid. Importantly, the integrals from the Steffen interpolation are virtually identical for the two grids, reflecting the excellent performance of the interpolation. For comparison, the 12-point Gauss-Legendre quadrature of $\alpha(i\omega)$ on the grid generated as described in Section 2 and the relevant cited references gives 36.05, in agreement with the Steffen-interpolated results beyond three significant figures.

Of course, the Steffen interpolation cannot be used beyond the highest frequency point of the grid. This is evident from the unphysical behavior of the standard grid interpolation

beyond 80 au seen in the left panel of Figure 1. It is therefore important to estimate the error from setting the grid cutoff around 80 au. For the fine grid, for which we assume the cutoff error to be negligible, the $\alpha(i\omega)$ integration gives 36.06 for the full frequency range (almost 1000 au), compared to 35.93 with a cutoff of $\omega = 81.92$. The grid truncation error is therefore only about 0.3% for the integral of α itself. For the integrations used to obtain C_6(K,K) and C_9(K,K,K), the truncation error turned out to be negligible already with the standard grid, because products of $\alpha(i\omega)$ go to zero even faster than α, and only the data points corresponding to low imaginary frequencies are sampled effectively. For the same reason, the grid spacing error may become somewhat amplified. For the standard grid, we obtain C_6(K,K) = 3901 from Steffen interpolation of $\alpha(i\omega)$ and integration according to Equation (1). The data from the fine grid gives 3895 instead, revealing an error of 0.2% with the standard grid mainly from the larger grid spacing at lower frequencies. For comparison, the 12-point Gauss-Legendre quadrature gives 3895, again at in agreement by three significant figures or better with the Steffen-interpolated results. Comparable relative agreements were obtained for C_9(K,K,K). Although the Gauss-Legendre quadrature appears to work at least as well as the integration of the Steffen interpolation function, it is easier to add results for additional frequencies to the interpolation procedure than adding points to the Gauss-Legendre grid. The latter requires re-calculating the polarizability at all grid points if the grid size is increased. We opted to proceed with the Steffen interpolation. The interpolation and cut-off errors are perfectly acceptable, given that the finite basis TDDFT calculations with approximate functionals entail other systematic errors. Dispersion coefficients from the present calculations, as reported throughout the remainder of this article, were therefore obtained from Steffen-interpolated data for the standard grid.

3.3 C_6(A,A) coefficients for alkali-metal atoms and some diatomic molecules

Plots of $\alpha(i\omega)$ are shown again in Figure 2, comparing Li, Na, and K. Additional plots for H_2, N_2, and CO are shown in Figure S1. The curves all behave qualitatively the same, although the frequency range at which the inflection point is reached extends significantly further for the diatomics, which also have a much smaller polarizability than the alkali atoms.

Table 2 collects the calculated C_6(A,A) for A = Li, Na, K and the diatomic molecules H_2, N_2 and CO. We also compare with other theoretical works. Our calculated C_6 are within the range of previously calculated values. For Li and Na, the C_6 coefficients are very similar to the those reported by Banerjee et al.,[4] which were obtained with a 'sum over states' TDDFT method, a non-hybrid functional, and Slater-type orbital basis sets. Furthermore, the C_6 coefficient for Li is nearly the same as the one calculated with a local response dis-

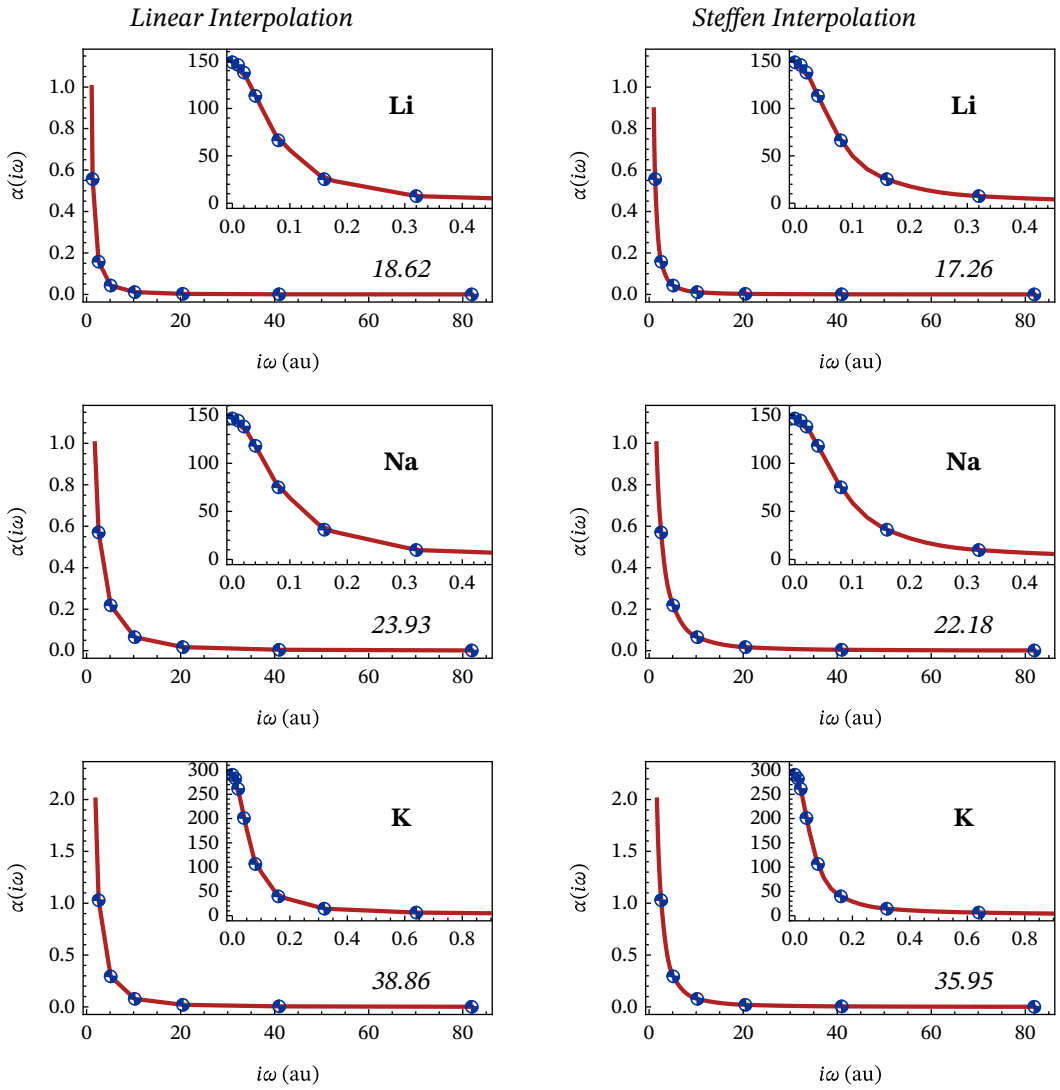

Figure 2: Polarizability at imaginary frequencies for the alkali-metal atoms Li, Na and K. Left: Linear interpolation Right: Cubic monotonic Steffen interpolation. The area under each interpolation is indicated by the numbers in italics.

persion method.[25] The C_6 coefficient obtained for K from our approach is very close to those reported by Gould and Bučko[19] (who used TDDFT and a 'bespoke' radial numerical code designed specifically for atoms), Chu and Dalgarno[23] (who likewise appeared to have used a code tailored for atoms, along with TDDFT) and Jiang et al.[54] Our C_6 coefficients of H_2 and N_2 are very similar to those evaluated previously by using dipole oscillator strength techniques, as in references 80 and 52 (*vide infra*). For CO, we also observe a good agreement between our approach and those calculated with dipole oscillator strength methods.[81] The value in the literature that matches best was obtained from all-electron TDDFT based method.[7]

3.4 C_6(A,B) and C_6(A,B_2) coefficients for alkali metal systems

For additional validation of our approach & implementation, we calculated C_6(A,B) and C_6(A,B_2) coefficients for the alkali metal atoms and compare them with available literature data[2–5,83,84] in Tables 3 and 4. Similar C_6(A,B) and C_6(A,B_2) coefficients are obtained in our approach compared to other studies, and the trends between different AB and AB_2 systems are faithfully reproduced, although in line with the noted low static polarizability for Li and

Table 2: Dispersion coefficients C_6(A,A) for the alkali-metal atoms and small diatomic molecules.[a]

System	C_6	Literature Data
Li	1195	1118,[b] 1426,[b] 1385,[e] 1386,[g] 1389,[j] 1388,[l] 1387,[m] 1439,[n] 1408,[o] 1100,[p] 1396,[q] 1392[r]
Na	1332	1244,[b] 1473,[b] 1527,[e] 1518,[g] 1540,[j] 1472,[l] 1639,[n] 1566,[o] 1037,[p] 1562,[q] 1518[r]
K	3901	3321,[b], 3590,[b] 3637,[e] 3574,[g] 3945,[j] 3813,[l] 4158,[n] 3914,[o] 3906,[q] 3923[r]
H_2	11.88	12.62,[c] 12.30,[c] 14.3,[f] 12.09,[h] 12.92,[k] 12.10[m]
N_2	72.14	75.63,[c] 71.46,[d] 77.2,[f] 73.43,[h] 74.09,[k] 73.3[m]
CO	78.38	89.14,[c] 73.96,[c] 83.8,[f] 81.31,[i] 79.75[k]

[a]This work. Equation (1) with CAM-B3LYP/Sadlej-pVTZ. [b]Reference 4. 'Sum over states' TDDFT method with Slater-type orbital (STO) basis. [c]Reference 62. Time-Dependent coupled Hartree-Fock (TDCHF) method with Gaussian-type orbitals (GTO) basis. [d]Reference 82. Time-Dependent coupled Hartree-Fock (TDCHF) method with tesseral harmonic GTO basis. [e]Reference 5. Perturbational approach, configuration interaction (CI) calculation using GTO basis. [f]Reference 1. TDDFT within the adiabatic local density approximation (ALDA) kernel using STO basis. [g]Reference 3. Configuration interaction (CI) + core polarization potential method with GTO basis. [h]Reference 80. Dipole oscillator strength approach. Numerical simulations. [i]Reference 81. Dipole oscillator strength approach. Numerical simulations. [j]Reference 83. Semi-empirical method. Numerical simulations. [k]Reference 7. All-electron TDDFT based method with the STO basis. [l]Reference 2. Second order perturbation expansion method. Numerical simulations. [m]Reference 52. Dipole oscillator strength approach. Numerical simulations. [n]Reference 84. Coupled-cluster theory with GTO basis. [o]Reference 19. TDDFT with a 'bespoke' radial numerical code. [p]Reference 25. Local response dispersion method. Numerical simulations. [q]Reference 54. Semi-empirical method using the oscillator strength distributions. Numerical simulations. [r]Reference 23. TDDFT with a code tailored for atoms. Numerical simulations.

Na from CAMB3LYP/Sadlej-pVTZ, the associated dispersion coefficients tend to be on the low end of the range of available values. We observe that our approach is in good agreement with the TDDFT sum-over-states method from reference 4 for Li-Na, Li-K, Na-K and K-K_2. In addition, the perturbational approach from Reference 5 also gives very similar coefficients, especially for the A-B_2 systems.

In reference 19, Gould and Bučko found very accurate C_6(A,B) coefficients by employing

Table 3: C_6(A,B) for alkali atom pairs

Method/Source	Li-Na	Li-K	Na-K
Equation (1)[a]	1258	2151	2258
Equation (3)[a]	1259	2153	2255
Ref. 2[b]	1427	2293	2348
Ref. 3[c]	1448	2219	2309
Ref. 4[d]	1448	2257	2288
Ref. 5[e]	1452	2238	2336
Ref. 83[f]	1460	2333	2443
Ref. 84[g]	1532	2441	2595

[a]This work. CAM-B3LYP/Sadlej-pVTZ. [b] Second order perturbation expansion method. Numerical simulations. [c] Configuration interaction (CI) + core polarization potential method with Gaussian-type orbitals (GTO) basis. [d] 'Sum over states' TDDFT method with Slater-type orbital (STO) basis. [e] Perturbational approach, configuration interaction (CI) using GTO basis. [f] Semi-empirical method. Numerical simulations. [g] Coupled-cluster (CC) theory with GTO basis.

Table 4: Dipole-dipole dispersion coefficients C_6(A,B_2) in atomic units. Comparison with other works.

A	B_2	This work[a]	Ref. 4[b]	Ref. 5[c]
Li	Li_2	1695	2108	1935
Li	Na_2	2065	2513	2394
Li	K_2	3535	3967	3791
Na	Li_2	1799	2148	2039
Na	Na_2	2196	2562	2524
Na	K_2	3728	4029	3966
K	Li_2	3034	3327	3102
K	Na_2	3698	3969	3838
K	K_2	6390	6302	6144

[a] Equation (1) with CAM-B3LYP/Sadlej-pVTZ. [b] 'Sum over states' TDDFT method with with Slater-type orbital (STO) basis. [c] Perturbational approach, configuration interaction (CI) using Gaussian-type orbital (GTO) basis.

the Moelwyn-Hughes[85] combining rule

$$C_6(A,B) = \frac{2C_6(A,A)C_6(B,B)}{\frac{\alpha^A(0)}{\alpha^B(0)}C_6(B,B) + \frac{\alpha^B(0)}{\alpha^A(0)}C_6(A,A)}. \quad (3)$$

Thus, if C_6(A,A) for different species A are already available, then the A–B dispersion coefficient can be estimated simply by calculating static polarizabilities. We calculated the C_6(A,B) coefficients according to Equation (3) for the alkali heterodimers, and compare the results with the ones obtained from Equation (1) in Table 3. Indeed, Equation (3) is seen to be very accurate, within the estimated error from the numerical integration of the interpolated polarizabilities using Equation (1). As a further test, for a system in which the polarizability and C_6 of species A and B differ by several orders of magnitude, C_6(K,H_2) was evaluated. Integration of the polarizability product according to Equation (1) with Steffen interpolation gave 139.7 au. Equation (3) gave 131.0 instead, using the same underlying polarizability data. The approximation from Equation (3) is still reasonable, but the percentage error from the approximation is evidently larger for K–H_2 than it is for the alkali–alkali dimer systems, and the use of Equation (1) is preferable. However, one may envision the use of a scaling correction,[19,23] based on ratios of $\alpha(\omega = 0)$ for species A and B, to correct for systematic errors in the calculated polarizability by employing a lower vs. higher level of theory. Of course, this would only be feasible for not too large systems where the scaling of the computational demands of a targeted high-level method (beyond the scaling of TDDFT linear response) is not impractical.

3.5 C_6(A,A) coefficients of other small molecules and larger systems

For further validation and testing of the approach & implementation, closed-shell molecules, such as ammonia, benzene, ethane, or buckminsterfullerene (C_{60}), as well as open-shell systems such as NH_2, O_2 or NO, were selected, based on the availability of literature data. We also included several more open-shell systems for which polarizabilities and C_6 coefficients have thus far not been reported, namely NO_2, perchlorotriphenylmethyl (PTM), and a persistent bicarbazole radical cation that we encountered in a recent study of chiral emitters.[73]

Table 5 displays the static polarizabilities, as well as the corresponding dispersion C_6 coefficients for the systems studied in this section. We also compare the results with the corresponding experimental polarizability (in case it is available in the literature) and theoretical C_6 coefficients from other studies. Note that our approach for other diatomic molecules and larger systems is in very good agreement with experiments and other literature data. For the most part, the available reference data are for closed-shell systems, for the reason that com-

putational methods for open-shell systems have traditionally been more limited, as already stated in the Introduction.

The reference data for O_2 and NO, which are both open-shell molecules, were obtained from discretized (pseudospectral) dipole oscillator strength distributions (DOSDs)[52] based on experimental data, or frequency-dependent polarizability data using Padé approximants also in conjunction with experimental data.[53] As such, these reference values can be con-

Table 5: Static polarizabilities (α) and dipole-dipole dispersion coefficients C_6(A,A) for selected molecules.[a]

System	α (calcd.)	α (expt.)	C_6	C_6 from Other Works
BeH	33.42 (32.72)[b]	-	170	
MgH	60.26 (62.66)[b]	-	471	
CaH	130.97 (134.34)[b]	-	1397	
CN	21.65 (20.50)[b]	-	116	
NH_2	12.39 (12.21)[b]	-	62.9	
NH_3	14.8 (15.6)[f]	15.0[c]	88.7	94.4,[f] 89.1,[j] 89.0,[h] 79.7[q]
C_2H_6	27.9 (30.7,[f] 29.4, [k] 27.6[k*])	30.2[c]	357	397,[f] 374.4,[k] 349.2[k], 381.8[n], 374.5[t]
C_6H_6	69.7 (68.2,[g] 70.0,[g*] 76.8,[o] 79.5,[o] 68.7[r])	68.7[d]	1765	1737,[g] 1773,[g*] 1730,[m] 1726,[p] 1956.8[q], 1779[r], 1874[t]
O_2	10.7	10.8[c]	60.7	61.6[h]
NO	11.6	-	68.1	69.7,[h] 69[l]
NO_2	19.7	-	160	
BCz	387.4	-	45.0[u]	
PTM	448.7	-	69.0[u]	
C_{60}	545.7 (538.0,[s] 543.1[s])	516±54[e]	99.0[u]	98.8,[u,i] 101.0,[u,g] 101.8,[u,g] 96.0[u,s], 97.1[u,t]

[a] This work, except where indicated otherwise. CAM-B3LYP/Sadlej-pVTZ. Calculated polarizabilities from the literature given in parentheses. [b]Reference 28. Møller-Plesset perturbation theory (MPPT) based on the quasi-energy derivative (QED) method using Gaussian-type orbital (GTO) basis. [c]Reference 86. [d]Reference 87. [e]Reference 88. [f]Reference 1. Time-dependent Density Functional Theory (TDDFT) within the adiabatic local density approximation (ALDA) kernel using Slater-type orbital (STO) basis. [g]Reference 12. Time-dependent Hartree-Fock (TDHF) with GTO basis. [g*]Reference 12. TDDFT with GTO basis. [h]Reference 52. Derived from experimental data; see text for details. [i]Reference 16. TDDFT with GTO basis. [j]Reference 89. Dipole oscillator strength distributions (DOSDs) method. Numerical simulations. [k]Reference 10. TDDFT with GTO basis. [k*]Reference 10. TDHF with GTO basis. [l]Reference 53. Derived from experimental data; see text for details. [m]Reference 14. TDDFT time propagation approach with ALDA. [n]Reference 90. DOSDs method. Numerical simulations. [o]Reference 91. HF level using GTO basis. [p]Reference 35. Symmetry-adapted perturbation theory (SAPT) with GTO basis. [q]Reference 38. Effective fragment potential (EFP2) method with GTO basis. [r]Reference 43. Coupled-cluster singles and doubles (CCSD) with GTO basis. [s]Reference 24. TDDFT with GTO basis. [t]Reference 45. Resolution-of-identity (RI) coupled-cluster singles and approximate doubles (RI-CC2) with GTO basis. [u]Values should be multiplied by 10^3.

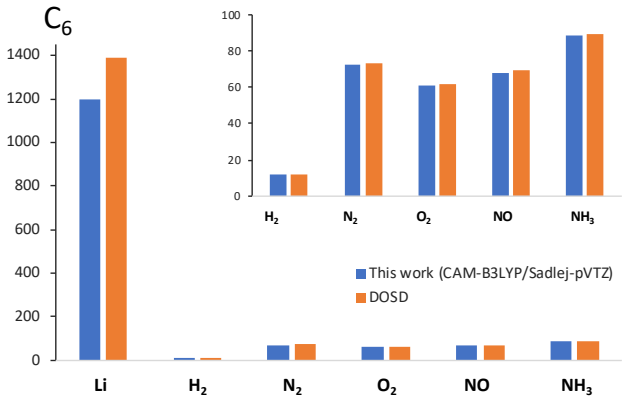

Figure 3: Dipole-dipole dispersion coefficients C_6(A,A) of selected systems obtained with TDDFT CAM-B3LYP/Sadlej-pVTZ, compared to DOSD-based results from Reference 52 reflecting experimental data.

sidered to represent experimental C_6 coefficients. Figure 3 compares the C_6 coefficients of selected small systems determined with our TDDFT approach versus data from Margoliash and Meath,[52] whose used the aforementioned DOSD approach. The Li data reflects the aforementioned underestimation of the calculated static polarizability with TDDFT CAM-B3LYP/Sadlej-pVTZ. Otherwise, the different results agree very well, both for closed-shell and open-shell molecules. Previous studies for C_6H_6 and C_{60} fullerene employed the aforementioned Gauss-Legendre quadrature.[12,24,43] We note that we obtain very similar data using the Steffen interpolation (see Table 5), showing that the integration accuracy is sufficient for these systems.

Given that the agreement of our data for C_{60} with literature data is also very good, we conclude that the NWChem implementation is capable of computing accurate linear response properties and dispersion coefficients for open- and closed-shell small, medium and larger systems.

3.6 C_9 coefficients

To demonstrate broader applicability of the method, additionally, C_9 coefficients were determined for alkali-metal atoms, diatomic molecules, and NH_3. For the case of three identical atoms, Midzuno and Kihara[92,93] derived an approximate expression for $C_9(A,A,A)$, which is given by

$$C_9(A,A,A) = \frac{3}{4}\alpha^A(0)\ C_6(\mathrm{A,A}), \tag{4}$$

along with a generalized approximate expression for C_9(A,B,C). We calculated the C_9 coefficients according to Equations (2) and (4), and compared to available literature data. Results

are collected in Tables 6, 7, 8, S2 and S3.

For the alkali metal atoms, Marinescu et al.[31] determined the three-body dispersion coefficients using nondegenerate perturbation theory and atomic hydrogen-like wavefunctions in the presence of pseudopotentials. Tang and coworkers[94] used oscillator strength sum rules, and Kang et al.[95] employed the combined l-dependent model potential with the linear variation method based on B-spline basis functions. In line with the C_6 coefficients, deviations between our approach and these studies is also observed for the C_9 coefficients of Li and Na (Tables 6 and 7), because of the underestimation of the polarizability of these atoms by CAM-B3LYP/Sadlej-pVTZ. For the K atom, we obtain very similar results to other data from the literature, which is also in line with the findings for the polarizability. The aforementioned correction scheme would seem to be useful, as it is easy to obtain the atomic polarizability with a large variety of high-level methods. Data for other functionals are discussed further below. Our limited set of data for the C_9(A,A,A) with A = Li, Na, or K confirms the excellent performance of the approximation provided by Equation (4).

For some diatomic molecules and NH_3, DOSD-derived data from Margoliash et al.[96] and, McDowell and Meath[97] are taken as references for our C_9(A,B,C) coefficients. Tables 8, S2

Table 6: Coefficients C_9(A,A,A) for alkali-metal atoms. Comparison with available literature data.

Atom	Eq. (2)[a]	Eq. (4)[a]	Ref. 31[b]	Ref. 94[c]	Ref. 95[d]
Li	133061	133362	170100	170620	170100
Na	145559	146453	175800	189200	175800
K	834151	849345	837500	831800	838200

[a] This work. CAM-B3LYP/Sadlej-pVTZ. [b] Nondegenerate perturbation theory. [c] Oscillator strength sum rules. [d] l-dependent model potential with the linear variation method.

Table 7: Triple-dipole dispersion coefficients C_9(A,B,C) for the combinations of alkali-metal atoms Li, Na and K. Comparison with available literature data.

A	B	C	This work[a]	Ref. 31[b]	Ref. 95[c]
Li	Li	Na	136760	171600	171700
Li	Li	K	244456	288400	288600
Na	Na	Li	140904	173500	173600
Na	Na	K	257346	292800	292900
K	K	Li	450780	490800	491100
K	K	Na	460777	492900	493500
Li	Na	K	250535	290400	290500

[a] This work. CAM-B3LYP/Sadlej-pVTZ. [b] Nondegenerate perturbation theory. [c] l-dependent model potential with the linear variation method.

and S3 show excellent agreement between the methods, apart from a now-expected underestimation when Li is involved because of the underestimation of the static polarizability by CAM-B3LYP/Sadlej-pVTZ. We also predict C_9 coefficients using other small and large systems for which these coefficients have not been reported thus far. Table S8 collects data for C_9(A,B,C) involving CO, CN, O_2, NO, NO_2, NH_2 and NH_3. Table 9 gathers our predictions for the C_9 involving larger systems, and additional calculated data can be found in Tables S4, S5, S6, and S7.

Table 8: Triple-dipole dispersion coefficients C_9(A,B,C) in atomic units involving Li, selected diatomic molecules, or NH_3. Comparison with DOSD-derived data from Margoliash et al.[96] and McDowell and Meath.[97]

A	B	C	This work[a]	DOSD[96]	DOSD[97]
H_2	N_2	CO	275.3	-	280.6
H_2	O_2	CO	248.3	-	252.1
H_2	CO	NO	266.5	-	272.1
N_2	H_2	Li	869.2	924.6	
N_2	CO	O_2	586.5	-	594.6
N_2	CO	NO	628.6	-	640.4
O_2	H_2	Li	782.4	830.8	-
O_2	N_2	Li	1734	1830	-
O_2	N_2	H_2	234.3	235.7	235.9
NO	H_2	Li	846.7	903.0	-
NO	N_2	Li	1876	1988	-
NO	N_2	H_2	251.4	254.2	254.5
NO	O_2	Li	1689	1787	-
NO	O_2	H_2	226.8	228.7	228.7
NO	O_2	N_2	537.8	541.0	541.5
CO	O_2	NO	568.0	-	576.7
NH_3	H_2	Li	1062	1121	-
NH_3	N_2	Li	2349	2465	-
NH_3	N_2	H_2	298.5	299.8	-
NH_3	O_2	Li	2115	2216	-
NH_3	O_2	H_2	269.1	269.4	-
NH_3	O_2	N_2	633.2	632.0	-
NH_3	NO	Li	2289	2408	-
NH_3	NO	H_2	289.0	290.0	-
NH_3	NO	N_2	679.0	681.2	-
NH_3	NO	O_2	613.2	613.5	-

[a] CAM-B3LYP/Sadlej-pVTZ.

3.7 Dependence of C_6 and C_9 coefficients on the functional

As seen, the polarizabilities and therefore the C_6 and C_9 coefficients depend on the accuracy of the dipole polarizabilities. The polarizability for Li and Na calculated with CAM-B3LYP/Sadlej-pVTZ underestimates the experimental reference values noticeably, which presumably translates into large deviations for the corresponding C_6 and C_9 coefficients. Therefore, other functionals that give static dipole polarizability values closer to the experiments were tested for verification. We evaluate here the results for Li and Na atoms, as they are the ones with largest error respect to other methods.

Table 10 lists the static polarizabilities, and the C_6 and C_9 coefficients for Li and Na varying the functional (and basis) employed. As expected, when the static polarizability is closer to experiments, the resulting C_6 and C_9 coefficients agree much better with other studies (compare with Tables 2 and 6). Excellent agreement is obtained with the LC functional LC-ωPBE for Li and with LC-PBE and the jorge-ATZP basis for Na. The table also shows results for C_6 and C_9 from the CAM-B3LYP/Sadlej-pVTZ calculations, scaled by the square or the cube, respectively, of the static polarizability results obtained with the different functionals relative to CAM-B3LYP/Sadlej-pVTZ. These are the dispersion coefficients corresponding to a global scaling correction for the $\alpha(i\omega)$ data set based on the static polarizability alone. The results are evidently improved over CAM-B3LYP/Sadlej-pVTZ, but not spot-on with the full results from the other functionals. This demonstrates that the dispersion of $\alpha(i\omega)$ relative to $\alpha(0)$ is also affected by the functional, and accurate results cannot be recovered simply by scaling $\alpha(i\omega)$ uniformly. Nonetheless, it is seen that the error in the static polarizability is a primary source of errors in the resulting C_6 and C_9 coefficients, whereas an incorrect prediction of the dispersion of α is a secondary source of errors. A simple scaling correction

Table 9: Triple-dipole dispersion coefficients C_9(A,B,C) involving C_2H_6, C_6H_6, BCz, PTM, and C_{60}.

A	B	C	CAM-B3LYP/Sadlej-pVTZ
C_2H_6	C_6H_6	BCz	192344
C_2H_6	C_6H_6	PTM	238168
C_2H_6	C_6H_6	C_{60}	284193
C_2H_6	BCz	PTM	1207920
C_2H_6	BCz	C_{60}	1442150
C_2H_6	PTM	C_{60}	1784310
C_6H_6	BCz	PTM	2772140
C_6H_6	BCz	C_{60}	3312130
C_6H_6	PTM	C_{60}	4091020
BCz	PTM	C_{60}	20825200

based on $\alpha(0)$ alone appears to be suitable for eliminating the leading-order errors.

Table 10: Static polarizabilities, dipole-dipole dispersion coefficients C_6(A,A) and triple-dipole C_9(A,A,A) coefficients for Li and Na using different functionals. The basis employed is Sadlej-pVTZ except where noted otherwise.[a]

System	Functional	α	C_6	scaled C_6	C_9	scaled C_9
Li	CAM-B3LYP	148.8	1195	-	133061	-
	LC-ωPBE (ω=0.4)	165.3	1406	1475	173983	182415
	LC-PBE0 (ω=0.3)	160.2	1343	1385	160956	166046
Na	CAM-B3LYP	146.6	1332	-	145559	-
	LC-PBE (ω=0.27)	164.8	1589	1683	195389	206780
	LC-PBE/jorge-ATZP (ω=0.27)	161.4	1541	1615	185900	194244

[a]See text for an explanation of the 'scaled' columns. The experimental α for Li and Na is 164 $\pm$ 3.0 and 159.2 $\pm$ 3.4, respectively.[78] See Tables 2 and 6 for C_6 and C_9 coefficients from other works.

4 Conclusions

We have demonstrated an efficient and accurate way to calculate dispersion coefficients C_6 and C_9 coefficients for closed- and open-shell molecules by using dynamic TDDFT complex-frequency linear response theory as implemented in the NWChem program. The dispersion coefficients were determined by the calculation of the corresponding polarizability at different imaginary frequencies with subsequent monotonic Steffen interpolation and integration. The results for closed- vs. open-shell species appear to be of similar quality. Systems with known large static correlation effects were not included in the test set on purpose, because Kohn-Sham (TD)DFT with commonly used approximations is expected to fail in such cases. Extensive comparisons with literature data were used to validate the polarizability and C_6 and C_9 coefficients. For motivation of new approaches for calculating dispersion coefficients of larger complexes with open-shell subsystems, and for future reference, we have predicted polarizabilities $\alpha(i\omega)$ as well as C_6 and C_9 coefficients for selected medium-size and larger compounds.

The results from the study indicate that a simple scaling of the static polarizabilities of the subsystems, based on comparisons of calculations at different levels of theory, would likely lead to improvements for cases where the static polarizability is predicted poorly by DFT. However, the dispersion of the polarizability along the imaginary frequency axis is also impacted by the functional/basis combination, such that a simple global scaling of $\alpha(i\omega)$ based on $\alpha(0)$ ratios is unlikely to recover the results from a higher-level method fully. However, the scaling appears to work well as a leading-order correction. The Steffen interpolation was shown to perform very well, and it can be recommended as an alternative to Gauss-Legendre quadrature for the integration used to obtain C_6, C_9, and in similar types of integrations where the underlying data can be assumed to decay in a monotonic fashion.

Supporting Information

Static polarizabilities of alkali-metal and diatomic molecules with different functionals and basis sets, polarizability of diatomic molecules using linear and Steffen interpolations, triple-dipole dispersion coefficients; C_9(A,A,A), C_9(A,A,B) and C_9(A,B,C) and, xyz coordinates.

Acknowledgments

We acknowledge the Center for Computational Research (CCR)[98] at the University at Buffalo for providing computational resources. This study has been supported by grant CHE-1855470

from the National Science Foundation.

References

(1) van Gisbergen, S. J. A.; Snijders, J. G.; Baerends, E. J. A density functional theory study of frequency-dependent polarizabilities and Van der Waals dispersion coefficients for polyatomic molecules. *J. Chem. Phys.* **1995**, *103*, 9347–9354.

(2) Marinescu, M.; Sadeghpour, H. R.; Dalgarno, A. Dispersion coefficients for alkali-metal dimers. *Phys. Rev. A* **1994**, *49*, 982–988.

(3) Müller, W.; Flesch, J.; Meyer, W. Treatment of intershell correlation effects in ab initio calculations by use of core polarization potentials. Method and application to alkali and alkaline earth atoms. *J. Chem. Phys.* **1984**, *80*, 3297–3310.

(4) Banerjee, A.; Autschbach, J.; Chakrabarti, A. Time dependent density functional theory calculation of the van der Waals coefficient C_6 of alkali-metal atoms Li, Na, K, alkali dimers Li_2, Na_2, K_2 and sodium clusters Na_n; and fullerene C_{60}. *Phys. Rev. A* **2008**, *78*, 032704–9.

(5) Spelsberg, D.; Lorenz, T.; Meyer, W. Dynamic multipole polarizabilities and long range interaction coefficients for the systems H, Li, Na, K, He, H-, H2, Li2, Na2, and K2. *J. Chem. Phys.* **1993**, *99*, 7845–7858.

(6) Andersson, Y.; Rydberg, H. Dispersion Coefficients for van der Waals Complexes, Including C60–C60. *Phys. Scr.* **1999**, *60*, 211–216.

(7) Kamal, C.; Ghanty, T. K.; Banerjee, A.; Chakrabarti, A. The van der Waals coefficients between carbon nanostructures and small molecules: A time-dependent density functional theory study. *J. Chem. Phys.* **2009**, *131*, 164708.

(8) Nguyen, H.-V.; de Gironcoli, S. Van der Waals coefficients of atoms and molecules from a simple approximation for the polarizability. *Phys. Rev. B* **2009**, *79*, 115105.

(9) Banerjee, A.; Harbola, M. K. Calculation of van der Waals coefficients in hydrodynamic approach to time-dependent density functional theory. *J. Chem. Phys.* **2002**, *117*, 7845–7851.

(10) Norman, P.; Jiemchooroj, A.; Sernelius, B. E. Polarization propagator calculations of the polarizability tensor at imaginary frequencies and long-range interactions for the noble gases and n-alkanes. *J. Chem. Phys.* **2003**, *118*, 9167–9174.

(11) Jiemchooroj, A.; Sernelius, B. E.; Norman, P. C_6 dipole-dipole dispersion coefficients for the *n*-alkanes: Test of an additivity procedure. *Phys. Rev. A* **2004**, *69*, 044701.

(12) Jiemchooroj, A.; Norman, P.; Sernelius, B. E. Complex polarization propagator method for calculation of dispersion coefficients of extended π-conjugated systems: The C6 coefficients of polyacenes and C60. *J. Chem. Phys.* **2005**, *123*, 124312.

(13) Jiemchooroj, A.; Norman, P.; Sernelius, B. E. Electric dipole polarizabilities and C6 dipole-dipole dispersion coefficients for sodium clusters and C60. *J. Chem. Phys.* **2006**, *125*, 124306.

(14) Marques, M. A. L.; Castro, A.; Malloci, G.; Mulas, G.; Botti, S. Efficient calculation of van der Waals dispersion coefficients with time-dependent density functional theory in real time: Application to polycyclic aromatic hydrocarbons. *J. Chem. Phys.* **2007**, *127*, 014107.

(15) Toulouse, J.; Rebolini, E.; Gould, T.; Dobson, J. F.; Seal, P.; Ángyán, J. G. Assessment of range-separated time-dependent density-functional theory for calculating C6 dispersion coefficients. *J. Chem. Phys.* **2013**, *138*, 194106.

(16) Kauczor, J.; Norman, P.; Saidi, W. A. Non-additivity of polarizabilities and van der Waals C6 coefficients of fullerenes. *J. Chem. Phys.* **2013**, *138*, 114107.

(17) Fransson, T.; Rehn, D. R.; Dreuw, A.; Norman, P. Static polarizabilities and C6 dispersion coefficients using the algebraic-diagrammatic construction scheme for the complex polarization propagator. *J. Chem. Phys.* **2017**, *146*, 094301.

(18) Tao, J.; Mo, Y.; Tian, G.; Ruzsinszky, A. Accurate van der Waals coefficients between fullerenes and fullerene-alkali atoms and clusters: Modified single-frequency approximation. *Phys. Rev. B* **2016**, *94*, 085126.

(19) Gould, T.; Bučko, T. C6 Coefficients and Dipole Polarizabilities for All Atoms and Many Ions in Rows 1–6 of the Periodic Table. *J. Chem. Theory Comput.* **2016**, *12*, 3603–3613.

(20) Andersson, Y.; Langreth, D. C.; Lundqvist, B. I. van der Waals Interactions in Density-Functional Theory. *Phys. Rev. Lett.* **1996**, *76*, 102–105.

(21) Tao, J.; Perdew, J. P.; Ruzsinszky, A. Accurate van der Waals coefficients from density functional theory. *PNAS* **2012**, *109*, 18–21.

(22) Osinga, V. P.; van Gisbergen, S. J. A.; Snijders, J. G.; Baerends, E. J. Density functional results for isotropic and anisotropic multipole polarizabilities and C6, C7, and C8 Van der Waals dispersion coefficients for molecules. *J. Chem. Phys.* **1997**, *106*, 5091–5101.

(23) Chu, X.; Dalgarno, A. Linear response time-dependent density functional theory for van der Waals coefficients. *J. Chem. Phys.* **2004**, *121*, 4083–4088.

(24) Brand, M.; Ahmadzadeh, K.; Li, X.; Rinkevicius, Z.; Saidi, W. A.; Norman, P. Size-dependent polarizabilities and van der Waals dispersion coefficients of fullerenes from large-scale complex polarization propagator calculations. *J. Chem. Phys.* **2021**, *154*, 074304.

(25) Ikabata, Y.; Nakai, H. Assessment of local response dispersion method for open-shell systems. *Chem. Phys. Lett.* **2013**, *556*, 386–392.

(26) Sekino, H.; Bartlett, R. J. Frequency dependent nonlinear optical properties of molecules. *J. Chem. Phys.* **1986**, *85*, 976–989.

(27) Aiga, F.; Itoh, R. Calculation of frequency-dependent polarizabilities and hyperpolarizabilities by the second-order Møller-Plesset perturbation theory. *Chem. Phys. Lett.* **1996**, *251*, 372–380.

(28) Kobayashi, T.; Sasagane, K.; Yamaguchi, K. Calculation of frequency-dependent polarizabilities for open-shell systems at the second-order Møller–Plesset perturbation theory level based on the quasi-energy derivative method. *Int. J. Quantum Chem.* **1997**, *65*, 665–677.

(29) Kooi, D. P.; Weckman, T.; Gori-Giorgi, P. Dispersion without Many-Body Density Distortion: Assessment on Atoms and Small Molecules. *J. Chem. Theo. Comput.* **2021**, *17*, 2283–2293.

(30) Jeziorski, B.; Moszynski, R.; Szalewicz, K. Perturbation Theory Approach to Intermolecular Potential Energy Surfaces of van der Waals Complexes. *Chem. Rev.* **1994**, *94*, 1887–1930.

(31) Marinescu, M.; Starace, A. F. Three-body dispersion coefficients for alkali-metal atoms. *Phys. Rev. A* **1997**, *55*, 2067–2074.

(32) Wormer, P. E. S.; Hettema, H.; Thakkar, A. J. Intramolecular bond length dependence of the anisotropic dispersion coefficients for H2-rare gas interactions. *J. Chem. Phys.* **1993**, *98*, 7140–7144.

(33) Porsev, S. G.; Derevianko, A. High-accuracy calculations of dipole, quadrupole, and octupole electric dynamic polarizabilities and van der Waals coefficients C6, C8, and C10 for alkaline-earth dimers. *J. Expt. Theor. Phys.* **2006**, *102*, 195–205.

(34) Akin-Ojo, O.; Szalewicz, K. Potential energy surface and second virial coefficient of methane-water from ab initio calculations. *J. Chem. Phys.* **2005**, *123*, 134311.

(35) Podeszwa, R.; Bukowski, R.; Szalewicz, K. Potential Energy Surface for the Benzene Dimer and Perturbational Analysis of $\pi-\pi$ Interactions. *J. Phys. Chem. A* **2006**, *110*, 10345–10354.

(36) Żuchowski, P. Interaction potential for the quintet state of the O2-O2 dimer from symmetry-adapted perturbation theory based on DFT description of monomers. *Chem. Phys. Lett.* **2008**, *450*, 203–209.

(37) Hodges, M. P.; Stone, A. J. A new representation of the dispersion interaction. *Mol. Phys.* **2000**, *98*, 275–286.

(38) Adamovic, I.; Gordon, M. S. Dynamic polarizability, dispersion coefficient C6 and dispersion energy in the effective fragment potential method. *Mol. Phys.* **2005**, *103*, 379–387.

(39) Patil, S. H.; Tang, K. T. Multipolar polarizabilities and two- and three-body dispersion coefficients for alkali isoelectronic sequences. *J. Chem. Phys.* **1997**, *106*, 2298–2305.

(40) Yan, Z.-C.; Babb, J. F.; Dalgarno, A.; Drake, G. W. F. Variational calculations of dispersion coefficients for interactions among H, He, and Li atoms. *Phys. Rev. A* **1996**, *54*, 2824–2833.

(41) Safronova, M. S.; Johnson, W. R. All-Order Methods for Relativistic Atomic Structure Calculations. *Adv. At. Mol. Opt. Phys.* **2008**, *55*, 191–233.

(42) Visentin, G.; Buchachenko, A. A. Polarizabilities, dispersion coefficients, and retardation functions at the complete basis set CCSD limit: From Be to Ba plus Yb. *J. Chem. Phys.* **2019**, *151*, 214302.

(43) Coriani, S.; Fransson, T.; Christiansen, O.; Norman, P. Asymmetric-Lanczos-Chain-Driven Implementation of Electronic Resonance Convergent Coupled-Cluster Linear Response Theory. *J. Chem. Theo. Comput.* **2012**, *8*, 1616–1628.

(44) Hättig, C.; Christiansen, O.; Jørgensen, P. Cauchy moments and dispersion coefficients using coupled cluster linear response theory. *J. Chem. Phys.* **1997**, *107*, 10592.

(45) Fedotov, D. A.; Coriani, S.; Hättig, C. Damped (linear) response theory within the resolution-of-identity coupled cluster singles and approximate doubles (RI-CC2) method. *J. Chem. Phys.* **2021**, *154*, 124110.

(46) Grimme, S. Accurate description of van der Waals complexes by density functional theory including empirical corrections. *J. Comput. Chem.* **2004**, *25*, 1463–1473.

(47) Grimme, S. Semiempirical GGA-type density functional constructed with a long-range dispersion correction. *J. Comput. Chem.* **2006**, *27*, 1787–1799.

(48) Grimme, S.; Antony, J.; Ehrlich, S.; Krieg, H. A consistent and accurate ab initio parametrization of density functional dispersion correction (DFT-D) for the 94 elements H-Pu. *J. Chem. Phys.* **2010**, *132*, 154104.

(49) Tkatchenko, A.; Scheffler, M. Accurate Molecular Van Der Waals Interactions from Ground-State Electron Density and Free-Atom Reference Data. *Phys. Rev. Lett.* **2009**, *102*, 073005.

(50) Tkatchenko, A.; DiStasio, R. A.; Car, R.; Scheffler, M. Accurate and Efficient Method for Many-Body van der Waals Interactions. *Phys. Rev. Lett.* **2012**, *108*, 236402.

(51) Bučko, T.; Lebègue, S.; Ángyán, J. G.; Hafner, J. Extending the applicability of the Tkatchenko-Scheffler dispersion correction via iterative Hirshfeld partitioning. *J. Chem. Phys.* **2014**, *141*, 034114.

(52) Margoliash, D.; Meath, W. J. Pseudospectral dipole oscillator strength distributions and some related two body interaction coefficients for H, He, Li, N, O, H2, N2, O2, NO, N2O, H2O, NH3, and CH4. *J. Chem. Phys.* **1978**, *68*, 1426–1431.

(53) Nielson, G. C.; Parker, G. A.; Pack, R. T. van der Waals interactions of π-state linear molecules with atoms. C6 for NO($X^2\,\pi$)interactions. *J. Chem. Phys.* **1976**, *64*, 2055–2061.

(54) Jiang, J.; Mitroy, J.; Cheng, Y.; Bromley, M. Effective oscillator strength distributions of spherically symmetric atoms for calculating polarizabilities and long-range atom–atom interactions. *At. Data Nucl. Data Tables* **2015**, *101*, 158–186.

(55) Schwerdtfeger, P. Atomic Static Dipole Poolarizabilities. In *Atoms, Molecules and Clusters in Electric Fields*; Maroulis, G., Ed.; IOS Press: Amsterdami, 2006; Chapter 1, 1–32.

(56) Aprà, E.; Bylaska, E. J.; de Jong, W. A.; Govind, N.; Kowalski, K.; Straatsma, T. P.; Valiev, M.; van Dam, H. J. J.; Alexeev, Y.; Anchell, J. et al. NWChem: Past, present, and future. *J. Chem. Phys.* **2020**, *152*, 184102 (27 pages).

(57) Autschbach, J. Time-dependent density functional theory for calculating origin-independent optical rotation and rotatory strength tensors. *ChemPhysChem* **2011**, *12*, 3224–3235.

(58) Autschbach, J. Computation of Optical Rotation using Time–Dependent Density Functional Theory. *Comput. Lett.* **2007**, *3*, 131–150.

(59) Abella, L.; Ludowieg, H. D.; Autschbach, J. Theoretical Study of the Raman Optical Activity Spectra of $[M(en)_3]^{3+}$ with M = Co, Rh. *Chirality* **2020**, *32*, 741–752.

(60) Aquino, F. W.; Schatz, G. C. Time-Dependent Density Functional Methods for Raman Spectra in Open-Shell Systems. *J. Phys. Chem. A* **2014**, *118*, 517–525.

(61) Casimir, H. B. G.; Polder, D. The Influence of Retardation on the London-van der Waals Forces. *Phys. Rev.* **1948**, *73*, 360–372.

(62) Rijks, W.; Wormer, P. E. S. Correlated van der Waals coefficients for dimers consisting of He, Ne, H2, and N2. *J. Chem. Phys.* **1988**, *88*, 5704–5714.

(63) NWChem quantum chemistry program package. URL `http://www.nwchem-sw.org` and `https://nwchemgit.github.io/` Accessed: 05/22.

(64) Yanai, T.; Tew, D. P.; Handy, N. C. A new hybrid exchange–correlation functional using the Coulomb-attenuating method (CAM-B3LYP). *Chem. Phys. Lett.* **2004**, *393*, 51–57.

(65) Sadlej, A. J. Medium-size polarized basis sets for high-level correlated calculations of molecular electric properties. *Collect. Czech. Chem. Commun.* **1988**, *53*, 1995.

(66) Hammond, J. R.; Govind, N.; Kowalski, K.; Autschbach, J.; Xantheas, S. S. Accurate dipole polarizabilities for water clusters n=2-12 at the coupled-cluster level of theory and benchmarking of various density functionals. *J. Chem. Phys.* **2009**, *131*, 214103.

(67) Schuchardt, K. L.; Didier, B. T.; Elsethagen, T.; Sun, L.; Gurumoorthi, V.; Chase, J.; Li, J.; Windus, T. L. Basis Set Exchange: A Community Database for Computational Sciences. *J. Chem. Inf. Model.* **2007**, *47*, 1045–1052.

(68) Pritchard, B. P.; Altarawy, D.; Didier, B.; Gibson, T. D.; Windus, T. L. A New Basis Set Exchange: An Open, Up-to-date Resource for the Molecular Sciences Community. *J. Chem. Inf. Model.* **2019**, 10.1021/acs.jcim.9b00725.

(69) Steffen, M. A simple method for monotonic interpolation in one dimension. *Astron. Astrophys.* **1990**, *239*, 443–450.

(70) *Mathematica* computer algebra software, Wolfram Research. URL `http://www.wolfram.com`, accessed 05/2022.

(71) Steffen interpolation on StackExchange. URL `https://mathematica.stackexchange.com/a/14040` accessed 05/2022.

(72) Huber, K.; Herzberg, G. Constants of Diatomic Molecules. In *NIST Chemistry WebBook, NIST Standard Reference Database Number 69*; Mallard, W. G.; Linstrom, P. J., Eds.; National Institute of Standards and Technology: Gaithersburg MD, 20899, 2005 data prepared by J.W. Gallagher and R.D. Johnson, III. URL: http://webbook.nist.gov.

(73) Kasemthaveechok, S.; Abella, L.; Jean, M.; Cordier, M.; Roisnel, T.; Vanthuyne, N.; Guizouarn, T.; Cador, O.; Autschbach, J.; Crassous, J.; Favereau, L. Axially and Helically Chiral Radical Bicarbazoles: SOMO-HOMO Level Inversion and Chirality Impact on the Stability of Mono- and Diradical Cations. *J. Am. Chem. Soc.* **2020**, *142*, 20409–20418.

(74) Adamo, C.; Barone, V. Toward reliable density functional methods without adjustable parameters: The PBE0 model. *J. Chem. Phys.* **1999**, *110*, 6158–6170.

(75) Weigend, F.; Ahlrichs, R. Balanced basis sets of split valence, triple zeta valence and quadruple zeta valence quality for H to Rn: Design and assessment of accuracy. *Phys. Chem. Chem. Phys.* **2005**, *7*, 3297–3305.

(76) Weigend, F. Accurate Coulomb-fitting basis sets for H to Rn. *Phys. Chem. Chem. Phys.* **2006**, *8*, 1057–1065.

(77) Frisch, M. J.; Trucks, G. W.; Schlegel, H. B.; Scuseria, G. E.; Robb, M. A.; Cheeseman, J. R.; Scalmani, G.; Barone, V.; Petersson, G. A.; Nakatsuji, H. et al. "Gaussian 16 Revision C.01", Gaussian, Inc., Wallingford CT, 2016. URL: www.gaussian.com.

(78) Molof, R. W.; Schwartz, H. L.; Miller, T. M.; Bederson, B. Measurements of electric dipole polarizabilities of the alkali-metal atoms and the metastable noble-gas atoms. *Phys. Rev. A* **1974**, *10*, 1131–1140.

(79) Autschbach, J.; Srebro, M. Delocalization error and 'functional tuning' in Kohn-Sham calculations of molecular properties. *Acc. Chem. Res.* **2014**, *47*, 2592–2602.

(80) Meath, W. J.; Kumar, A. Reliable isotropic and anisotropic dipolar dispersion energies, evaluated using constrained dipole oscillator strength techniques, with application to interactions involving H2, N2, and the rare gases. *Int. J. Quantum Chem.* **1990**, *38*, 501–520.

(81) Kumar, A.; Meath, W. J. Reliable isotropic and anisotropic dipole properties, and dipolar dispersion energy coefficients, for CO evaluated using constrained dipole oscillator strength techniques. *Chem. Phys.* **1994**, *189*, 467–477.

(82) Visser, F.; Wormer, P. E. S.; Stam, P. Time-dependent coupled Hartree-Fock calculations of multipole polarizabilities and dispersion interactions in van der Waals dimers consisting of He, H2, Ne, and N2. *J. Chem. Phys.* **1983**, *79*, 4973–4984.

(83) Maeder, F.; Kutzelnigg, W. Natural states of interacting systems and their use for the calculation of intermolecular forces: IV. Calculation of van der Waals coefficients between one- and two-valence-electron atoms in their ground states, as well as of polarizabilities, oscillator strength sums and related quantities, including correlation effects. *Chemical Phys.* **1979**, *42*, 95–112.

(84) Stanton, J. F. Calculation of C_6 dispersion constants with coupled-cluster theory. *Phys. Rev. A* **1994**, *49*, 1698–1703.

(85) Kramer, H. L.; Herschbach, D. R. Combination Rules for van der Waals Force Constants. *J. Chem. Phys.* **1970**, *53*, 2792–2800.

(86) Bridge, N. J.; Buckingham, A. D.; Linnett, J. W. The polarization of laser light scattered by gases. *Proc. R. Soc.* **1966**, *295*, 334–349.

(87) Okruss, M.; Müller, R.; Hese, A. High-resolution ultraviolet laser spectroscopy on jet-cooled benzene molecules: Ground and excited electronic state polarizabilities determined from static Stark effect measurements. *J. Chem. Phys.* **1999**, *110*, 10393–10402.

(88) Antoine, R.; Dugourd, P.; Rayane, D.; Benichou, E.; Broyer, M.; Chandezon, F.; Guet, C. Direct measurement of the electric polarizability of isolated C60 molecules. *J. Chem. Phys.* **1999**, *110*, 9771–9772.

(89) Zeiss, G.; Meath, W. J. Dispersion energy constants C 6(A, B), dipole oscillator strength sums and refractivities for Li, N, O, H2, N2, O2, NH3, H2O, NO and N2O. *Mol. Phys.* **1977**, *33*, 1155–1176.

(90) Jhanwar, B.; Meath, W. J. Pseudo-spectral dipole oscillator strength distributions for the normal alkanes through octane and the evaluation of some related dipole-dipole and triple-dipole dispersion interaction energy coefficients. *Mol. Phys.* **1980**, *41*, 1061–1070.

(91) Perez, J. J.; Sadlej, A. J. Ab initio calculations of the polarizability of some aromatic molecules. *J. Mol. Struct.: THEOCHEM* **1996**, *371*, 31–36.

(92) Midzuno, Y.; Kihara, T. Non-additive Intermolecular Potential in Gases I. van der Waals Interactions. *J. Phys. Soc. Jpn* **1956**, *11*, 1045–1049.

(93) Kihara, T. Intermolecular Forces and Equation of State of Gases. *Adv. Chem. Phys.* **1957**, *1*, 267–307.

(94) Tang, L.-Y.; Yan, Z.-C.; Shi, T.-Y.; Babb, J. F.; Mitroy, J. The long-range non-additive three-body dispersion interactions for the rare gases, alkali, and alkaline-earth atoms. *J. Chem. Phys.* **2012**, *136*, 104104.

(95) Kang, S.; Ding, C.-K.; Chen, C.-Y.; Wu, X.-Q. High-Order Dispersion Coefficients for Alkali-metal Atoms. *Commun. Theor. Phys.* **2013**, *60*, 73–79.

(96) Margoliash, D. J.; Proctor, T. R.; Zeiss, G.; Meath, W. J. Triple-dipole energies for H, He, Li, N, O, H2, N2, O2, NO, N2O, H2O, NH3 and CH4 evaluated using pseudo-spectral dipole oscillator strength distributions. *Mol. Phys.* **1978**, *35*, 747–757.

(97) McDowell, S. A. C.; Meath, W. J. Isotropic and anisotropic triple-dipole dispersion energy coefficients for three-body interactions involving He, Ne, Ar, Kr, Xe, H2, N2, CO, O2 and NO. *Mol. Phys.* **1997**, *90*, 713–720.

(98) Center for Computational Research, University at Buffalo. URL `http://hdl.handle.net/10477/79221`. Accessed 11/2019.

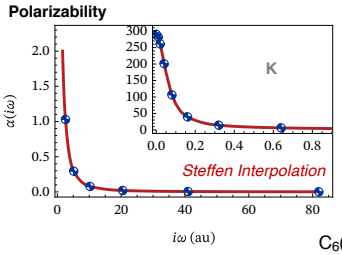

Dynamic TD-DFT Linear Response Theory

For Closed- and Open-Shell Atoms and Molecules

Dispersion Coefficients

$$C_6(A,B) = \frac{3}{\pi}\int_0^\infty \alpha^A(i\omega)\alpha^B(i\omega)d\omega$$

$$C_9(A,B,C) = \frac{3}{\pi}\int_0^\infty \alpha^A(i\omega)\alpha^B(i\omega)\alpha^C(i\omega)d\omega$$